Interference and parity blockade in transport through a Majorana box

Maximilian Nitsch [1,*] Rubén Seoane Souto [1,2,†] and Martin Leijnse [1,2,‡]

[1]*Division of Solid State Physics and NanoLund, Lund University, S-22100 Lund, Sweden*
[2]*Center for Quantum Devices, Niels Bohr Institute, University of Copenhagen, DK-2100 Copenhagen, Denmark*

A Majorana box—two topological superconducting nanowires coupled via a trivial superconductor—is a building block in devices aiming to demonstrate non-Abelian physics, as well as for topological quantum computer architectures. We theoretically investigate charge transport through a Majorana box and show that current can be blocked when two Majoranas couple to the same lead, fixing their parity. In direct analogy to a Pauli spin blockade in spin qubits, this parity blockade can be used for fast and high-fidelity qubit initialization and readout, as well as for current-based measurements of decoherence times. Furthermore, we demonstrate that transport can distinguish between a clean Majorana box and a disordered box with additional unwanted Majorana or Andreev bound states.

Introduction. Topological *p*-wave superconductors host Majorana bound states (MBSs) [1–7] at edges and defects, which have nonlocal and non-Abelian properties. Semiconductor nanowires are one of the most promising systems for creating and detecting MBSs, where a combination of spin-orbit coupling, proximity-induced superconductivity, and external magnetic field can lead to *p*-wave superconductivity [8,9]. By now, many experiments have observed zero-bias conductance peaks, consistent with MBSs at the nanowire ends (see Refs. [10–15] for a few examples; similar results have been obtained also in other MBS platforms). However, nontopological states provide an alternative explanation for most of the experimental observations [16–24].

A measurement of the non-Abelian properties of MBSs is still missing, but would provide definite evidence of a topological superconducting phase, constituting at the same time a first step towards topological quantum computing. One promising path towards a demonstration of non-Abelian physics uses repeated measurements of MBS pairs to perform topologically protected qubit operations [25], with a possibility to move towards a scalable quantum computer platform [26–29]. A simple building block for these technologies is the Majorana box qubit [30], where a qubit is encoded in four MBSs with overall parity fixed by a large charging energy. Qubit readout can be done by charge sensing of a quantum dot coupled to two MBSs [31–34], or by measuring the interference of cotunneling currents when the box is connected to

external leads [35]. Furthermore, coupling the Majorana box to more than two leads enables measurements of the topological Kondo effect [36–39], and networks of coupled Majorana boxes exhibit additional interesting transport physics [40–45].
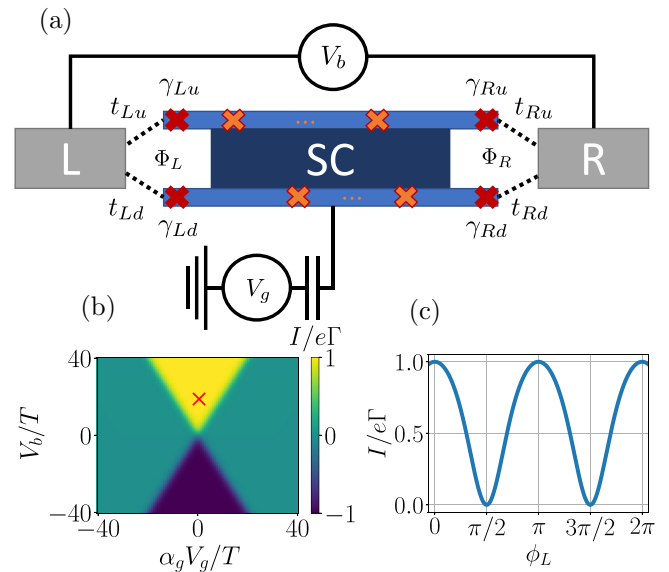

FIG. 1. (a) Sketch of Majorana box, where two topological superconducting wires (blue), connected by a nontopological superconductor (dark blue), host four end MBSs (red crosses, operators γ_{rm}). Disorder might lead to additional unwanted MBSs (orange crosses). The box is tunnel coupled (amplitudes t_{rm}) to two normal leads (L and R), subject to a voltage bias V_b. Magnetic fluxes Φ_L, Φ_R are threaded through the loops associated with leads L, R and cause relative phase differences ϕ_L, ϕ_R between t_{Lu} and t_{Ld}, t_{Ru}, and t_{Rd}. A gate voltage V_g controls the equilibrium number of electrons on the Majorana box. (b) Current I through the Majorana box as a function of V_b and V_g with the remaining parameters specified in the text. (c) I at $V_g = 0$ V, $V_b = 20T$ red cross in (a) as a function of ϕ_L at $\phi_R = 0$.

*maximilian.nitsch@ftf.lth.se
†ruben.seoane_souto@ftf.lth.se
‡martin.leijnse@ftf.lth.se

In this Letter, we develop and employ a quantum master equation approach to investigate charge transport through a Majorana box where the source and drain contacts couple to two MBSs each [see Fig. 1(a)]. We show that the same mechanism that allows quantum-dot-based parity readout [31,32,34] induces a parity blockade in our transport setup, where the current is quenched and the qubit is stuck in a well-defined state. This is in close analogy to the Pauli spin blockade in double quantum dot spin qubits [46,47]. Just as the Pauli spin blockade, a parity blockade can simplify various important qubit experiments. Fast and high-fidelity qubit initialization can be achieved by driving a current through the Majorana box which quickly gets stuck in the blocked state. The same principle can be used for readout, by applying a bias voltage such that an electron tunnels if the system is not in the blocking state. Single-shot readout can then be accomplished by charge detection on the box. Alternatively, measuring the current resulting from repeated operations provides an averaged readout. We solve the quantum master equation analytically for the clean box with four end MBSs and numerically for a disordered Majorana box with additional unwanted MBSs or topologically trivial Andreev bound states (ABSs). We show that the qubit coherence time can be read off from the remnant steady-state current in the blocking regime. This measurement requires neither fast manipulation, nor fast readout, only a dc transport measurement. Finally, we explain how to distinguish the clean Majorana box from the disordered system with additional MBSs or ABSs inside the box.

Model and transport theory. We consider the Majorana box transport setup sketched in Fig. 1(a). Two topological superconducting nanowires are connected by a conventional (nontopological) superconductor and are tunnel coupled to electrically biased normal source and drain contacts. The Hamiltonian is $H = H_{\mathrm{MB}} + H_{\mathrm{res}} + H_T$. The Majorana box is described by ($e = \hbar = k_B = 1$)

$$H_{\mathrm{MB}} = \sum_{m=u,d} \frac{i}{2} \varepsilon_m \gamma_{Lm} \gamma_{Rm} + E_C (N - n_g)^2 + H_{\mathrm{MB}}^{\mathrm{dis}}, \quad (1)$$

where γ_{rm} are MBS operators and ε_m is the overlap between MBSs in the same wire (our results remain qualitatively the same in the presence of additional overlaps between MBSs in different wires), E_C is the charging energy, N counts the number of electrons (including Cooper pairs) on the Majorana box, and n_g is the background charge controlled by the gate voltage V_g, $n_g = \alpha_g V_g$ with a gate lever arm α_g. $H_{\mathrm{MB}}^{\mathrm{dis}}$ describes a number of additional unwanted MBSs [orange crosses in Fig. 1(a)] induced by disorder, which may overlap with each other and with the edge MBSs γ_{rm} (see specific examples below). In this low-energy Hamiltonian we neglect the quasiparticle states above the superconducting gap.

The lead Hamiltonian is $H_{\mathrm{res}} = \sum_r H_r$, with $H_r = \sum_k \xi_{rk} c_{rk}^\dagger c_{rk}$, where the $c_{rk}^\dagger$ create spinless electrons in lead $r = L, R$ with energies ξ_{rk}. We assume the leads to remain in thermal equilibrium at temperature T and chemical potential $\mu_{L,R} = \pm V_b/2$. The tunneling between the leads and Majorana box is described by

$$H_T = \sum_{rmk} \gamma_{rm}(t_{rm} c_{rk} - t_{rm}^* c_{rk}^\dagger) + H_T^{\mathrm{dis}}, \quad (2)$$

with tunnel amplitudes t_{rm} which we take to be energy independent (wideband limit). We include magnetic fluxes Φ_L, Φ_R threaded through the loops formed by leads L, R and the end MBSs [Fig. 1(a)] by adding a phase $\phi_r = 2\pi \Phi_r / \Phi_0$ to the upper tunnel amplitude of the left and right leads, $t_{ru} = |t_{ru}| e^{i\phi_r}$, $t_{rd} = |t_{rd}|$, where Φ_0 is the flux quantum. The amplitude for a tunneling-induced transition between two many-body eigenstates a and b of the Majorana box is related to the tunnel matrix element $T_r^{ab} = \sum_{m=u,d} \langle a | \gamma_{rm} | b \rangle$. The typical timescale of electron tunneling is then given by the tunnel rates $\Gamma_r^{ab} = 2\pi \nu_r |T_r^{ab}|^2$, where we take the density of states ν_r to be energy-independent within the bandwidth chosen as $D = 100T$. Unless stated otherwise, we will throughout this Letter consider all tunnel amplitudes and densities of states to be equal, $t_{rm} = t$ and $\nu_r = \nu$, and define $\Gamma = 2\pi \nu |t|^2$. H_T^{dis} describes the tunnel coupling of the disorder-induced MBSs to the leads.

Let us comment on two model assumptions which will be important for the results and which place some constraints on an experimental realization. First, the way γ_{ru} and γ_{rd} couple to the same lead channel in Eq. (2) is only strictly correct for an effectively one-dimensional (1D) lead, but is a good approximation whenever tunneling from γ_{ru} and γ_{rd} occurs into points of the lead separated by less than the Fermi wavelength. Second, considering spinless lead electrons is valid either when the magnetic field needed to induce the topological superconducting phase has fully spin polarized the lead electrons around the Fermi level, or when the spin directions associated with allowed tunneling into γ_{ru} and γ_{rd} are aligned [48] (which is the case for two identical wires).

Quantum master equations. We focus on the regime of weak tunneling, $\Gamma \ll T$, but strong electron-electron interaction E_C. Then it is appropriate to use a quantum master equation for the reduced density matrix ρ of the Majorana box:

$$\partial_t \rho = -i[H_{\mathrm{MB}}, \rho] + W\rho. \quad (3)$$

The quantum master equation consists of a unitary time evolution determined by H_{MB} and a dissipative part introduced by the attached leads. We diagonalize the Majorana box Hamiltonian in Eq. (1) to obtain the many-body eigenstates $|a_i\rangle$ and solve the master equation for the stationary state reduced density matrix $\rho_{a_1 a_2}$ and current I, where tunneling is treated in leading-order perturbation theory. We emphasize that, because of the near-degenerate ground state, it is important to solve for the full nondiagonal density matrix. All results presented below are obtained within a first-order von Neumann quantum master equation [49] (equivalent to real-time diagrammatics in first order [50–52]). We have cross-checked that other approximations [53,54] provide similar results, and details are given in the Supplemental Material (SM) [55].

Because of the large E_C we consider only two charge states, arbitrarily denoted by $N = 0$ and $N = 1$, corresponding to the total parity of the MBSs being even or odd. We tune V_g such that the two parity sectors are almost degenerate. The density matrix is diagonal in total parity, and a term in the master equation describing an electron tunneling onto or out of the Majorana box connects the two parity sectors.

Parity blockade. We first consider the clean box with $H_{\mathrm{MB}}^{\mathrm{dis}} = 0$ and $\varepsilon_m = 0$. The current I as a function of V_b and

V_g for $\phi_L = \phi_R = 0$ [Fig. 1(b)] shows the Coulomb blockade pattern characteristic of transport through quantum dots [56]. The current is finite for V_b, V_g such that there are available electrons in one contact that can tunnel into the Majorana box ($N \to N + 1$) and available empty states in the other contact that can accept electrons tunneling out of the box ($N + 1 \to N$). Otherwise, current is suppressed by charging effects (Coulomb blockade).

For the remainder of this Letter, we fix the voltages within the conducting regime [at the point marked by the red cross in Fig. 1(b)]. We now vary ϕ_L [see Fig. 1(c)] and find $I(\phi_L) \propto \cos^2 \phi_L$, meaning that the current is blocked for $\phi_L = (2n + 1)\frac{\pi}{2}, n \in Z$. To understand the blockade, we construct fermion operators using the two left and the two right MBSs: $f_L = (\gamma_{Lu} + i\gamma_{Ld})/2$, $f_R = (\gamma_{Rd} + i\gamma_{Ru})/2$. The eigenstates of the number operators $\hat{n}_r = f_r^\dagger f_r$, $r = L, R$, $|n_L n_R\rangle$, are also eigenstates of H_{MB} when $\varepsilon_m = 0$ and $H_{MB}^{dis} = 0$. Note that the even eigenstates, $|0_L 0_R\rangle$ and $|1_L 1_R\rangle$, are degenerate, and so are the odd eigenstates, $|0_L 1_R\rangle$ and $|1_L 0_R\rangle$. With this choice of basis and in this simple limit, the density matrix is diagonal. At the chosen voltages, electrons tunnel into the Majorana box from lead L and out to lead R. For a current to flow, the state of the Majorana box must change according to $|0_L 0_R\rangle \to |1_L 0_R\rangle \to |1_L 1_R\rangle \to |0_L 1_R\rangle \to |0_L 0_R\rangle \to \cdots$ (electron tunnels in from the left, out to the right, in from the left, out to the right, etc.). Note that because the number states $n_{L,R}$ are not charge eigenstates, it is possible to, for example, switch from $n_L = 1$ to $n_L = 0$ by an electron *entering* the box from contact L. Taking the tunneling term that adds an electron from the left lead in Eq. (2), and writing it in terms of the left/right fermion operator, we obtain

$$H_{T,L} \to t \sum_k [c_k(e^{i\phi_L} + i)f_L^\dagger + c_k(e^{i\phi_L} - i)f_L], \quad (4)$$

which is not Hermitian as we neglect tunneling terms from the box into the left lead. For $\phi_L = \pi/2$ the second term in Eq. (4) vanishes, which results in the transition $|1_L 1_R\rangle \to |0_L 1_R\rangle$ being suppressed. Therefore, the system becomes trapped in the blocking state $|1_L 1_R\rangle$ and no current can flow. For $\phi_L = 3\pi/2$ the blocking state is instead $|0_L 0_R\rangle$. Reversing V_b or changing ϕ_R at the right lead causes blocking instead in an odd state ($|0_L 1_R\rangle$ or $|1_L 0_R\rangle$). We note that, in direct analogy with the Pauli spin blockade [46,57], this parity blockade can be used for fast and high-fidelity initialization of a Majorana box qubit in any of the blocking states, as well as for readout in the corresponding basis.

Finite overlap between MBSs. We now move on to investigate how the blockade is lifted and how to read off qubit lifetimes from the remnant current $I_{rem} = \min_{\phi_L}[I(\phi_L)]$ in the blocked regime. First, we note that the blockade is lifted for asymmetric tunnel couplings to the upper/lower MBSs. We will quantify this more explicitly below and for now assume $t_{Lu} = t_{Ld}$. For now we keep the assumption $H_{MB}^{dis} = 0$ but take $\varepsilon_m \neq 0$. Then the eigenstates are $|n_u n_d\rangle$ rather than $|n_L n_R\rangle$, associated with the up/down fermions with operators $f_m = (\gamma_{Lm} + i\gamma_{Rm})/2$ for $m = u, d$. The eigenenergies $E_{n_u n_d}$ within each parity sector are split by the MBS overlap, $2\Delta_e = E_{11} - E_{00} = \varepsilon_u + \varepsilon_d$ and $2\Delta_o = E_{01} - E_{10} = \varepsilon_u - \varepsilon_d$. Moreover, the coupling to the leads introduces a Lamb shift given

by

$$H_{LS} = \Gamma I_P \begin{pmatrix} \sigma_x(\sin\phi_L + \sin\phi_R) & 0_2 \\ 0_2 & -\sigma_x(\sin\phi_L - \sin\phi_R), \end{pmatrix}$$
$$(5)$$

proportional to the principle value integrals I_P (see Refs. [55,58,59]).

We can write the master equation in terms of the probability $p_{e/o}$ to be in the even/odd sector, and a pseudospin $\vec{s}_{e/o}$ that describes the density matrix within each sector, where we choose the z axis to be along $|n_L n_R\rangle$. In the SM [55], we derive Bloch-like equations for the pseudospin and show that the current is given by

$$I = 2e\,\Gamma(p_e + \sin\phi_L\, s_e^z). \quad (6)$$

Without MBS overlaps, $s_{e,o}^z$ are decoupled from $s_{e,o}^{x,y}$. Finite overlaps correspond to a magnetic field of strength $\Delta_{e,o}$ along the x direction. In leading-order perturbation theory, $\Delta_{e,o}$ induces an additional loss term of magnitude $\Delta^2/\Gamma^2(1 + I_P^2)$ in the master equation for $\partial_t s_e^z$ at $\phi_L = \pi/2$. The blocking state corresponds to $p_e = 1 - \frac{1}{2}\Delta^2/\Gamma^2(1 + I_P^2)$, $s_e^z = -1 + \Delta^2/\Gamma^2(1 + I_P^2)$, resulting in a current $I_{rem} = e\Delta_e^2/\Gamma(1 + I_P^2)$. This result can be generalized to any mechanism that allows parity to escape from the left Majorana pair ($n_L = 0 \to n_L = 1$) without changing the total charge on the Majorana box. If the parity escape rate is $\tilde{\Delta}/\hbar$, the resulting remnant current is $I_{rem} = e\tilde{\Delta}^2/\Gamma(1 + I_P^2)$ in the blocking regime. Interestingly, a larger tunnel coupling to the leads enhances the lifetime of the blocking state and suppresses current. Thus, even though a measurement of the remnant current directly gives the inverse lifetime of the blocking state $1/\tau = I_{rem}/e$, this is not the same as that for the isolated Majorana box. The Lamb shift is not experimentally accessible and experiments can only extract the decay rate of the coupled Majorana box qubit $\tilde{\Delta}_{coup} \equiv \tilde{\Delta}/(1 + I_P^2)^{1/2}$ which is always smaller but of the same order of magnitude as the decay rate $\tilde{\Delta}$ of the isolated Majorana box. To measure $\tilde{\Delta}_{coup}$ one should first extract Γ from the current in the nonblocked regime [see Fig. 1(c)], and then measure $\tilde{\Delta}_{coup}^2/\Gamma$ from the current in the blocked regime.

Finite overlap with unwanted MBSs. We illustrate this with a specific model for a disordered device containing unwanted MBSs. We assume that these MBSs are uncoupled to the leads, $H_T^{dis} = 0$, and

$$H_{MB}^{dis} = \frac{i}{2} \sum_{m=u,d} \sum_{r=L,R} \tilde{\varepsilon}_{rm}\gamma_{rm}\tilde{\gamma}_{rm} + \Omega_m\tilde{\gamma}_{Lm}\tilde{\gamma}_{Rm}, \quad (7)$$

where the $\tilde{\gamma}$'s are four additional disorder-induced MBSs with couplings Ω_m between each other and couplings $\tilde{\varepsilon}_{rm}$ to the end MBSs. For $\tilde{\varepsilon}_{Lu} \gg \tilde{\varepsilon}_{Ld}, \Omega_m$, the relevant parity escape rate is $\tilde{\Delta} \approx (\tilde{\varepsilon}_{Lu} \pm \tilde{\varepsilon}_{Ld})/2 \approx \tilde{\varepsilon}_{Lu}/2$. Figure 2 shows the current as a function of Γ. For $\Gamma \ll \tilde{\Delta}$ the current is proportional to Γ, it peaks at $\Gamma \approx \tilde{\Delta}$, and then decays with larger Γ as $\tilde{\Delta}_{coup}^2/\Gamma$ (dotted black line in Fig. 2).

Asymmetric tunnel couplings. We also introduce deviations from the ideal blocked situation $|t_{Ld}/t_{Lu}| = 1 - \delta_t$, $\phi_L = \frac{\pi}{2} + \delta_\phi$, $\delta = \sqrt{\delta_t^2 + \delta_\phi^2}$. These deviations lead to a contribution to the current that is linear in Γ (dashed black line) which dominates I_{rem} for $\Gamma > \tilde{\Delta}_{coup}/2\delta$ [55]. In particular, the different scaling in Γ makes it possible to distinguish experimentally
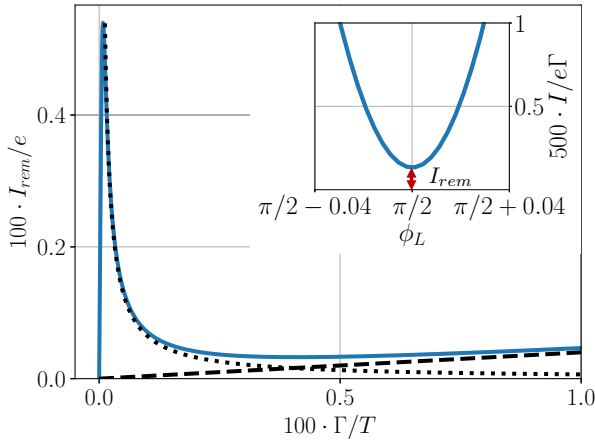
FIG. 2. Inset: Lifting of the blockade at $\phi_L = \frac{\pi}{2}$ for $\varepsilon_{Lu} = 2 \times 10^{-4}T$ and $\delta_t = 10^{-2}$. The main plot shows I_{rem} as a function of Γ for $\delta_t = \delta_\phi = 10^{-2}$. After a sharp increase linear in Γ until $\Gamma \approx \tilde{\Delta}_{\text{coup}}$, I_{rem} decreases as $e \tilde{\Delta}_{\text{coup}}^2 / \Gamma$ (black dotted line) before it increases again as $2e \delta^2 \Gamma$ (black dashed line).

FIG. 3. (a) Escape rate mechanisms leading to I_{rem} for the clean box (blue), the disordered box (red), and the ABS box (green). (b) I_{rem} as a function of ϕ_R at $\phi_L = \frac{\pi}{2}$ and $\Gamma = 10^{-2}T$ renormalized by $I_{\text{rem}}(\phi_R = 0)$ for all three box models in line colors that match colors in (a). The overlaps are chosen as ε_U, $\varepsilon_{Lu} = 10^{-5}T$. For each model we plot I_{rem} for the perfectly fine-tuned setting (solid lines), deviation in the fine-tuned tunneling $\delta_t = 10^{-4}$ (dotted lines), mismatch in tunneling to the left/right lead $\Gamma_R = \Gamma_L/2$ (dashed-dotted lines), and a very large overlap ε_U, $\varepsilon_{Lu} = 10^{-3}T$ (dashed lines).

between a remnant current caused by an escape rate ($I \propto 1/\Gamma$) compared to one due to finite δ ($I \propto \Gamma$).

Distinguishing clean from disordered box. Now we move on to showing that the phase dependence of the Lamb shift offers the possibility to distinguish between the clean box with only four MBSs in total, and the disordered box with additional MBSs or ABSs [Fig. 3(a)]. We model each ABS as two closely spaced MBSs which both couple to the leads by

$$H_T^{\text{dis}} = \sum_{rmk} \tilde{\gamma}_{rm}(t_{rm}c_{rk} - t_{rm}^* c_{rk}^\dagger), \qquad (8)$$

but with no overlaps with the MBSs on the other side of the box, Ω_m, $\epsilon_U = 0$. For each of these three cases, we block the current from the left lead with $\phi_L = \frac{\pi}{2}$ and investigate the dependence of I_{rem} on ϕ_R. Figure 3(b) shows that the result is qualitatively different for the clean box (blue lines) compared with the disordered box (red lines) and ABS box (green lines), and this difference is robust to various parameter choices (different line styles).

In the case of the clean box the Lamb shifts introduced by both leads either add up ($\phi_R = \frac{\pi}{2}$) or subtract ($\phi_R = \frac{3\pi}{2}$) [see Eq. (5)]. This leads to a decrease, respectively increase, in I_{rem}. This qualitative dependence is stable under all investigated parameter settings. For a large overlap, there appears a peak at $\phi_R = \frac{\pi}{2}$, which corresponds to an additional blockade at the right lead interfering with the blockade at the left lead.

For the disordered box with additional MBSs or ABSs, the line shape is qualitatively different, with only very narrow dips (width $\propto \tilde{\Delta}_{\text{coup}}/\Gamma$) around $\phi_R = \frac{\pi}{2}, \frac{3\pi}{2}$. They mark a transition from a blockade at the left lead to a blockade at the right lead with a smaller overlap/escape rate.

The qualitative difference of $I_{\text{rem}}(\phi_R)$ is due to the different escape mechanism from the parity blocked state to the next pair of MBSs [see Fig. 3(a)]. In the clean box this nearest
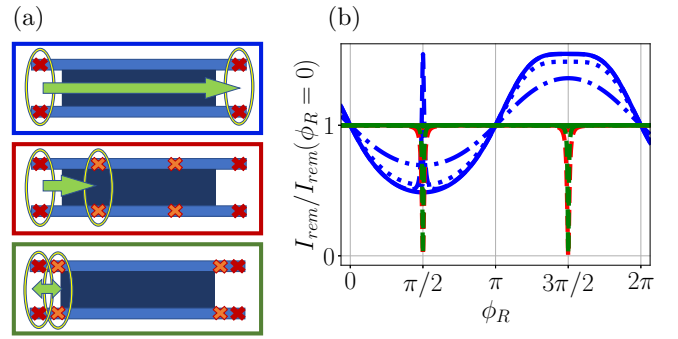
pair of MBSs is connected to the right lead. Accordingly, the adjustment of the Lamb shift via ϕ_R affects the remnant current. But for the disordered and ABS boxes the nearest pair is located in the inner part/at the left end of the setup. There is no connection to the right lead and accordingly no dependence on the phase ϕ_R.

Conclusions. We have used a quantum master equation approach to investigate transport through a Majorana box coupled to normal leads. There is a blocking regime, where the Majorana box becomes trapped in a well-defined state and the current is suppressed. In analogy with the Pauli spin blockade, this parity blockade can be used for qubit initialization and readout, as well as for measuring qubit coherence times from dc transport. We believe that this can become a key enabling technique for a first generation of MBS qubit experiments, where single-shot readout might be challenging due to limited control or short qubit coherence times. Furthermore, the proposed setup makes it possible to experimentally distinguish between a clean Majorana box and a box with additional disorder-induced MBSs or ABSs.

If we assume that $T = 100$ mK ≈ 10 μeV, the choice of parameters used in this Letter corresponds to $V_b \approx 200$ μV and $\Gamma \approx 1$ μeV ≈ 200 MHz. It is then possible to measure qubit lifetimes $< 1/\Gamma \approx 5$ ns.

In our model, the parity lifetime is limited by MBS overlaps, but we expect that if some other form of relaxation or decoherence dominates (e.g., quasiparticle poisoning), the proposed measurement of the remnant current will instead reveal the corresponding timescale.

[1] A. Y. Kitaev, Phys. Usp. **44**, 131 (2001).

[2] C. Nayak, S. H. Simon, A. Stern, M. Freedman, and S. Das Sarma, Rev. Mod. Phys. **80**, 1083 (2008).

[3] J. Alicea, Rep. Prog. Phys. **75**, 076501 (2012).

[4] M. Leijnse and K. Flensberg, Semicond. Sci. Technol. **27**, 124003 (2012).

[5] R. Aguado, Riv. Nuovo Cimento **40**, 523 (2017).

[6] C. W. J. Beenakker, Sci-Post Phys. Lect. Notes **1**, 15 (2020).

[7] K. Flensberg, F. von Oppen, and A. Stern, Nat. Rev. Mater. **6**, 944 (2021).

[8] Y. Oreg, G. Refael, and F. von Oppen, Phys. Rev. Lett. **105**, 177002 (2010).

[9] R. M. Lutchyn, J. D. Sau, and S. Das Sarma, Phys. Rev. Lett. **105**, 077001 (2010).

[10] V. Mourik, K. Zuo, S. M. Frolov, S. R. Plissard, E. P. A. M. Bakkers, and L. P. Kouwenhoven, Science **336**, 1003 (2012).

[11] M. T. Deng, C. L. Yu, G. Y. Huang, M. Larsson, P. Caroff, and H. Q. Xu, Nano Lett. **12**, 6414 (2012).

[12] A. D. K. Finck, D. J. Van Harlingen, P. K. Mohseni, K. Jung, and X. Li, Phys. Rev. Lett. **110**, 126406 (2013).

[13] M. T. Deng, S. Vaitiekėnas, E. B. Hansen, J. Danon, M. Leijnse, K. Flensberg, J. Nygård, P. Krogstrup, and C. M. Marcus, Science **354**, 1557 (2016).

[14] F. Nichele, A. C. C. Drachmann, A. M. Whiticar, E. C. T. O'Farrell, H. J. Suominen, A. Fornieri, T. Wang, G. C. Gardner, C. Thomas, A. T. Hatke, P. Krogstrup, M. J. Manfra, K. Flensberg, and C. M. Marcus, Phys. Rev. Lett. **119**, 136803 (2017).

[15] R. M. Lutchyn, E. P. Bakkers, L. P. Kouwenhoven, P. Krogstrup, C. M. Marcus, and Y. Oreg, Nat. Rev. Mater. **3**, 52 (2018).

[16] E. Prada, P. San-Jose, and R. Aguado, Phys. Rev. B **86**, 180503(R) (2012).

[17] G. Kells, D. Meidan, and P. W. Brouwer, Phys. Rev. B **86**, 100503(R) (2012).

[18] C. Moore, C. Zeng, T. D. Stanescu, and S. Tewari, Phys. Rev. B **98**, 155314 (2018).

[19] C. Reeg, O. Dmytruk, D. Chevallier, D. Loss, and J. Klinovaja, Phys. Rev. B **98**, 245407 (2018).

[20] O. A. Awoga, J. Cayao, and A. M. Black-Schaffer, Phys. Rev. Lett. **123**, 117001 (2019).

[21] A. Vuik, B. Nijholt, A. R. Akhmerov, and M. Wimmer, SciPost Phys. **7**, 061 (2019).

[22] H. Pan and S. Das Sarma, Phys. Rev. Res. **2**, 013377 (2020).

[23] E. Prada, P. San-Jose, M. W. A. de Moor, A. Geresdi, E. J. H. Lee, J. Klinovaja, D. Loss, J. Nygård, R. Aguado, and L. P. Kouwenhoven, Nat. Rev. Phys. **2**, 575 (2020).

[24] R. Hess, H. F. Legg, D. Loss, and J. Klinovaja, Phys. Rev. B **104**, 075405 (2021).

[25] P. Bonderson, M. Freedman, and C. Nayak, Phys. Rev. Lett. **101**, 010501 (2008).

[26] S. Vijay, T. H. Hsieh, and L. Fu, Phys. Rev. X **5**, 041038 (2015).

[27] L. A. Landau, S. Plugge, E. Sela, A. Altland, S. M. Albrecht, and R. Egger, Phys. Rev. Lett. **116**, 050501 (2016).

[28] S. Plugge, L. A. Landau, E. Sela, A. Altland, K. Flensberg, and R. Egger, Phys. Rev. B **94**, 174514 (2016).

[29] T. Karzig, C. Knapp, R. M. Lutchyn, P. Bonderson, M. B. Hastings, C. Nayak, J. Alicea, K. Flensberg, S. Plugge, Y. Oreg, C. M. Marcus, and M. H. Freedman, Phys. Rev. B **95**, 235305 (2017).

[30] S. Plugge, A. Rasmussen, R. Egger, and K. Flensberg, New J. Phys. **19**, 012001 (2017).

[31] M. I. K. Munk, J. Schulenborg, R. Egger, and K. Flensberg, Phys. Rev. Res. **2**, 033254 (2020).

[32] J. F. Steiner and F. von Oppen, Phys. Rev. Res. **2**, 033255 (2020).

[33] T. B. Smith, M. C. Cassidy, D. J. Reilly, S. D. Bartlett, and A. L. Grimsmo, PRX Quantum **1**, 020313 (2020).

[34] J. Schulenborg, M. Burrello, M. Leijnse, and K. Flensberg, Phys. Rev. B **103**, 245407 (2021).

[35] L. Fu, Phys. Rev. Lett. **104**, 056402 (2010).

[36] B. Béri and N. R. Cooper, Phys. Rev. Lett. **109**, 156803 (2012).

[37] M. R. Galpin, A. K. Mitchell, J. Temaismithi, D. E. Logan, B. Béri, and N. R. Cooper, Phys. Rev. B **89**, 045143 (2014).

[38] E. Eriksson, C. Mora, A. Zazunov, and R. Egger, Phys. Rev. Lett. **113**, 076404 (2014).

[39] F. Buccheri and R. Egger, in *Strongly Coupled Field Theories for Condensed Matter and Quantum Information Theory*, edited by A. Ferraz, K. S. Gupta, G. W. Semenoff, and P. Sodano (Springer, Cham, 2020), pp. 131–153.

[40] B. Béri, Phys. Rev. Lett. **110**, 216803 (2013).

[41] A. Altland and R. Egger, Phys. Rev. Lett. **110**, 196401 (2013).

[42] L. Herviou, K. Le Hur, and C. Mora, Phys. Rev. B **94**, 235102 (2016).

[43] K. Michaeli, L. A. Landau, E. Sela, and L. Fu, Phys. Rev. B **96**, 205403 (2017).

[44] M. Gau, S. Plugge, and R. Egger, Phys. Rev. B **97**, 184506 (2018).

[45] J. I. Väyrynen, A. E. Feiguin, and R. M. Lutchyn, Phys. Rev. Res. **2**, 043228 (2020).

[46] K. Ono, D. G. Austing, Y. Tokura, and S. Tarucha, Science **297**, 1313 (2002).

[47] R. Hanson, L. P. Kouwenhoven, J. R. Petta, S. Tarucha, and L. M. K. Vandersypen, Rev. Mod. Phys. **79**, 1217 (2007).

[48] M. Kjaergaard, K. Wölms, and K. Flensberg, Phys. Rev. B **85**, 020503(R) (2012).

[49] G. Kiršanskas, J. N. Pedersen, O. Karlström, M. Leijnse, and A. Wacker, Comput. Phys. Commun. **221**, 317 (2017).

[50] J. König, H. Schoeller, and G. Schön, Phys. Rev. Lett. **78**, 4482 (1997).

[51] M. Leijnse and M. R. Wegewijs, Phys. Rev. B **78**, 235424 (2008).

[52] H. Schoeller, Eur. Phys. J.: Spec. Top. **168**, 179 (2009).

[53] F. Nathan and M. S. Rudner, Phys. Rev. B **102**, 115109 (2020).

[54] G. Kiršanskas, M. Franckié, and A. Wacker, Phys. Rev. B **97**, 035432 (2018).

[55] See Supplemental Material at http://link.aps.org/supplemental/10.1103/PhysRevB.106.L201305 for an analytical derivation of the main results in this Letter, which includes Refs. [60–62].

[56] L. P. Kouwenhoven, D. G. Austing, and S. Tarucha, Rep. Prog. Phys. **64**, 701 (2001).

[57] J. Danon and Y. V. Nazarov, Phys. Rev. B **80**, 041301(R) (2009).

[58] H.-P. Breuer and F. Petruccione, *The Theory of Open Quantum Systems* (Oxford University Press, Oxford, UK, 2002).

[59] K. Ptaszyński and M. Esposito, Phys. Rev. Lett. **122**, 150603 (2019).

[60] D. E. Evans, Commun. Math. Phys. **54**, 293 (1977).

[61] D. E. Evans and H. Hanche-Olsen, J. Funct. Anal. **32**, 207 (1979).

[62] D. Manzano, AIP Adv. **10**, 025106 (2020).